1987 ACC, Minneapolis, MN.

CONTROL OF HIGH-PURITY DISTILLATION COLUMNS FROM A ROBUSTNESS VIEWPOINT

Sigurd Skogestad
Manfred Morari

California Institute of Technology
Chemical Engineering, 206-41
Pasadena, CA 91125

Abstract

A realistic study of the LV-control of a high-purity distillation column is presented. Linear controllers designed based on a linearized model of the plant are found to yield acceptable performance also when there is model-plant mismatch. The mismatch can be caused by uncertainty on the manipulated inputs, nonlinearity and variations in reboiler and condenser holdup. The presence of input uncertainty makes the use of a steady-state decoupler unacceptable. The effect of nonlinearity is strongly reduced by using the logarithm of the compositions. A simple diagonal PI-controller is not sensitive to model-plant mismatch, but yields a response with a sluggish return to steady-state.

1. INTRODUCTION

In this paper we study the high-purity distillation column in Table 1 using reflux (L) and boilup (V) as manipulated inputs to control the top (y_D) and bottom (x_B) compositions. This column was analyzed previously by the authors (Skogestad and Morari, 1986a), but the objective of that paper was to study general properties of ill-conditioned plants rather than distillation column control. The goal of this paper is to provide a realistic control design and simulation study for the column. To be realistic at least the issues of 1) uncertainty and 2) nonlinearity must be addressed.

Uncertainty

Skogestad and Morari (1986a) showed that the closed-loop system may be extremely sensitive to input uncertainty when the LV-configuration is used. In particular, inverse-based controller were found to display severe robustness problems. In this paper the uncertainty is explicitly taken into account when designing and analyzing the controllers by using the Structured Singular Value (μ) introduced by Doyle (1982). We also find that μ provides a much easier way of comparing and analyzing the effect of various combinations of controllers, uncertainty and disturbances than the traditional simulation approach.

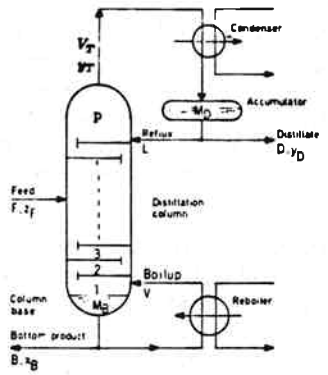

Figure 1. Two product distillation column

Nonlinearity

High-purity distillation columns are known to be strongly nonlinear (e.g. Moczek et al., 1963), and any realistic study should take this into account. Our approach is to base the controller design on a linear model. The effect of nonlinearity is taken care of by analyzing this controller for linearized models at *different operating points*. Furthermore, all simulations are based on the full nonlinear model.

Logarithmic Compositions

In another paper (Skogestad and Morari, 1987a) we study the dynamic behavior of distillation columns in general. One conclusion from that paper is that the high-frequency behavior is only weakly affected by operating conditions when the scaled transfer matrix is considered

$$\begin{pmatrix} dy_D^S \\ dx_B^S \end{pmatrix} = G^S \begin{pmatrix} dL \\ dV \end{pmatrix} \quad , G^S = \begin{pmatrix} \frac{1}{1-y_D^o} & 0 \\ 0 & \frac{1}{1-x_B^o} \end{pmatrix} G \quad (1)$$

All plant models and controllers in this paper are for the scaled plant. G^S is obtained by scaling the outputs with respect to the amount of impurity in each product

---

Binary separation, constant molar flows, feed liquid.

Column Data:

Relative Volatility	$\alpha = 1.5$
No. of theoretical trays	$N = 40$
Feed tray (1=reboiler)	$N_F = 21$
Feed composition	$z_F = 0.5$

Operating variables:

	A	C
$y_D =$	0.99	0.90
$x_B =$	0.01	0.002
$D/F =$	0.500	0.555
$L/F =$	2.706	2.737

Steady-state gains (unscaled compositions):

$$\begin{pmatrix} dy_D \\ dx_B \end{pmatrix} = G(0) \begin{pmatrix} dL/F \\ dV/F \end{pmatrix}$$

$$G(0) = \begin{matrix} \\ \text{A} \\ \\ \\ \\ \\ \text{C} \end{matrix} \begin{matrix} \\ \begin{pmatrix} 0.878 & -0.864 \\ 1.082 & -1.096 \end{pmatrix} \\ \\ \\ \\ \\ \begin{pmatrix} 1.604 & -1.602 \\ .01865 & -.02148 \end{pmatrix} \end{matrix}$$

Table 1. Steady-state data for distillation column at operating points A and C.

$$y_D^S = \frac{y_D}{1-y_D^o}, \quad x_B^S = \frac{x_B}{x_B^o} \tag{2}$$

Here x_B^o and y_D^o are the compositions at the nominal operating point. This relative scaling is automatically obtained by using logarithmic compositions

$$Y_D = \ln(1-y_D), \quad X_B = \ln x_B \tag{3}$$

because

$$dY_D = -\frac{dy_D}{1-y_D}, \quad dX_B = \frac{dx_B}{x_B} \tag{4}$$

Furthermore, the use of logarithmic compositions (Y_D and X_B) effectively eliminates the effect of nonlinearity at high frequency (Skogestad and Morari, 1987a) and also reduces its effect at steady-state (Skogestad and Morari, 1987b). For control purposes the high frequency behavior (initial response) is of principal importance. Consequently, if logarithmic compositions are used we expect a linear controller to perform satisfactorily also when we are far removed from the nominal operating point for which the controller was designed. Another objective of this paper is to confirm that this is indeed true.

2. THE DISTILLATION COLUMN

Steady-state data for the distillation column are given in Table 1. The following simplifying assumptions are made: a1) binary separation, a2) constant relative volatility, a3) constant molar flows and a4) constant holdups on all trays and perfect level control. The last assumption results in immediate flow response, that is, we are neglecting flow dynamics. This is somewhat unrealistic, and in order to avoid unrealistic controllers, we will add "uncertainty" at high frequency to include the effect of neglected flow dynamics when designing and analyzing the controllers (see Section 3).

We investigate the column at two different operating points. At the nominal operating point, A, both products are high-purity and $1-y_D^o = x_B^o = 0.01$. Operating point C is obtained by increasing D/F from 0.500 to 0.555 which yields a less pure top product and a purer bottom product; $1-y_{DC}^o = 0.10$ and $x_{BC}^o = 0.002$ (subscript C denotes operating point C while no subscript denotes operating point A). We will study the column for the following two assumptions regarding reboiler and condenser holdup:

Case 1: Almost negligible condenser and reboiler holdup ($M_D/F = M_B/F = 0.5$ min).

Case 2: Large condenser and reboiler holdup ($M_D/F =$ 32.1 min, $M_B/F = 11$ min).

These two cases will be denoted by subscripts 1 and 2, respectively. The holdup on each tray inside the column is $M_i/F = 0.5$ min in both cases.

2.1 Modelling

Nominal operating point (A). A 41st order linear model for the columns is easily derived based on the data given in Table 1 (see Skogestad and Morari, 1987a)

$$\begin{pmatrix} dy_D \\ dx_B \end{pmatrix} = G(s) \begin{pmatrix} dL \\ dV \end{pmatrix} \tag{5}$$

The scaled steady-state gain matrix is

$$G^S(0) = \begin{bmatrix} 87.8 & -86.4 \\ 108.2 & -109.6 \end{bmatrix} \tag{6}$$

which yields the following values for the condition number and the 1,1-element in the RGA

$$\gamma(G^S(0)) = \frac{\bar{\sigma}(G^S(0))}{\underline{\sigma}(G^S(0))} = 141.7 \qquad \lambda_{11}(G^S(0)) = 35.1$$

However, $\gamma(G^S)$ and $\lambda_{11}(G^S)$ are much smaller at high frequencies as seen from Fig.2.

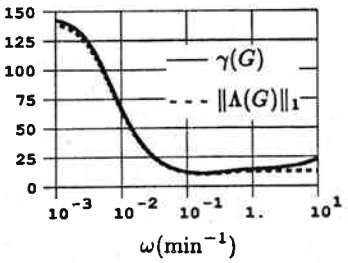

Fig. 2. Column A, Case 1 ($G = G_1^S$). The condition number of the plant is about 10 times lower at high frequencies than at steady state.

Case 1. For the case of negligible reboiler and condenser holdup he following simple two time-constant model yields an excellent approximation of the 41st order linear model (Skogestad and Morari, 1987a).

$$\text{Model 1}: \quad G_1^S(s) = \begin{pmatrix} \frac{87.8}{1+\tau_1 s} & -\frac{87.8}{1+\tau_1 s} + \frac{1.4}{1+\tau_2 s} \\ \frac{108.2}{1+\tau_1 s} & \frac{-108.2}{1+\tau_1 s} - \frac{1.4}{1+\tau_2 s} \end{pmatrix} \tag{8}$$

with $\tau_1 = 194$ min and $\tau_2 = 15$ min. $G_1(s)$ uses two time constants: τ_1 is the time constant for changes in the external flows. It corresponds to the dominant time constant and may be estimated, for example, by using the inventory time constant of Moczek et al. (1963). τ_2 is the time constant for changes in internal flows (simultaneous change in L and V with constant product rates, D and B) and can be estimated by matching the high-frequency behavior as shown by Skogestad and Morari (1987a). The simple model (8) matches the observed variation in condition number with frequency (Fig.2).

Case 2. In order to obtain a low-order model for this case we performed a model reduction (Balanced Realization, Moore (1981)) on the full 41st order model. A good approximation, $G_2(s)$, was obtained with a 5th order model.

Operating point C. We will return with a discussion of the model for this case in Section 6 when we also discuss the control of the plant.

2.2 Simulations

The design and analysis of the controller are based on the linear models $G_1(s)$ and $G_2(s)$. However, except for the four simplifying assumptions a1-a4 stated above, all simulations are carried out with the full nonlinear model. To get a realistic evaluation of the controllers input uncertainty must be included. Simulations are therefore shown both with and without 20% uncertainty with respect to the change of the two inputs. The following uncertainties are used

$$\Delta L = (1+\Delta_1)\Delta L_c, \quad \Delta_1 = 0.2$$
$$\Delta V = (1+\Delta_2)\Delta V_c, \quad \Delta_2 = -0.2 \qquad (9)$$

Here ΔL and ΔV are the actual changes in manipulated flow rates, while ΔL_c and ΔV_c are the desired values as computed by the controller. $\Delta_1 = -\Delta_2$ was chosen to represent the worst combination of the uncertainties (Skogestad and Morari, 1986b).

3. CONTROL THEORY

3.1 Robust performance and robust stability

The objective of using feedback control is to keep the controlled outputs (in our case y_D and x_B) "close" to their desired setpoints. What is meant by "close" is more precisely defined by the performance specifications. These performance requirements should be satisfied in spite of unmeasured disturbances and model-plant mismatch (uncertainty). Consequently, the ultimate goal of the controller design is to achieve Robust Performance (RP): The performance specification should be satisfied for the worst case combination of disturbances and model-plant mismatch. The implications of this requirement are easier to understand if we consider some subobjectives which have to be satisfied in order to achieve this goal:

Nominal Stability (NS): The closed loop system with the controller applied to the (nominal) plant model has to be stable.

Nominal Performance (NP): We will define performance in terms of the weighted sensitivity function S:

$$NP \quad \Leftrightarrow \quad \bar{\sigma}(w_P S) \le 1 \quad \forall\omega, \quad S = (I+GC)^{-1} \qquad (10)$$

The weight w_P is used to specify the frequency range over which the errors are to be small. To get consistency with the notation used below define $\bar{\sigma}(w_P S) = \mu(N_{NP})$ such that (10) becomes

$$NP \quad \Leftrightarrow \quad \mu(N_{NP}) \le 1 \quad \forall\omega \qquad (11)$$

where $N_{NP} = w_P S$, and μ is computed with respect to the structure of a "full" matrix Δ_P.

Robust Stability (RS). The closed loop system must remain stable for all possible plants as defined by the uncertainty description. For example, assume there is uncertainty with respect to the actual magnitude of the manipulated inputs (which is always the case!). The possible plants, G_p, are then given by

$$G_p = G(I+\Delta_I), \qquad \Delta_I = \begin{pmatrix} \Delta_1 & 0 \\ 0 & \Delta_2 \end{pmatrix} \qquad (12)$$

where $\Delta_i(s)$ is the uncertainty for input i. We will consider the case when the magnitude of uncertainty is equal for both inputs

$$|\Delta_i| \le |w_I(j\omega)|, \quad i = 1,2 \qquad (13)$$

The robust stability requirement can be checked using μ. In this particular case (Skogestad and Morari, 1986a)

$$RS \quad \Leftrightarrow \quad \mu(N_{RS}) \le 1, \quad \forall\omega \qquad (14)$$

where $N_{RS} = w_I CGS$ and μ is computed with respect to the diagonal 2×2 matrix Δ_I.

Robust Performance (RP): For RP we require (10) to be satisfied when G is replaced by any of the possible perturbed plants G_p as defined by the uncertainty description (12).

$$RP \quad \Leftrightarrow \quad \bar{\sigma}(w_P(I+G_pC)^{-1}) \le 1 \quad \forall\omega, \quad \forall G_p \qquad (15)$$

The structured singular value μ provides a computationally useful condition for checking whether (15) is satisfied:

$$RP \quad \Leftrightarrow \quad \mu(N_{RP}) \le 1, \quad \forall\omega \qquad (16a)$$

where

$$N_{RP} = \begin{pmatrix} w_I CSG & w_I CS \\ w_P SG & w_P S \end{pmatrix} \qquad (16b)$$

and μ is computed with respect to the structure $diag\{\Delta_I, \Delta_p\}$ where Δ_I is 2×2 diagonal matrix and Δ_P is a full 2×2 matrix.

3.2 The RGA

Let $\times$ denote element-by-element multiplication. The RGA of the matrix G (Bristol, 1966) is defined as

$$\Lambda(G) = G \times (G^{-1})^T \qquad (17)$$

The RGA is independent of input and output scaling. The RGA of the plant is commonly used as a tool for selecting control configurations for distillation columns (Shinskey, 1984). However, in this paper we will make use of the RGA of the controller as a measure of a system's sensitivity to input uncertainty (Skogestad and Morari, 1986b).

Again, consider uncertainty on the plant inputs as given by (12). The loop transfer matrix, G_pC, for the perturbed plant may be written in terms of its nominal value, GC:

$$G_pC = GC(I + C^{-1}\Delta_I C) \qquad (18)$$

G_pC is closely related to performance because of (15). For 2×2 plants the error term $C^{-1}\Delta_I C$ in (18) may be expressed in terms of the RGA of the controller:

$$C^{-1}\Delta_I C = \begin{bmatrix} \lambda_{11}\Delta_1 + \lambda_{21}\Delta_2 & \lambda_{11}\frac{c_{12}}{c_{11}}(\Delta_1 - \Delta_2) \\ -\lambda_{11}\frac{c_{21}}{c_{22}}(\Delta_1 - \Delta_2) & \lambda_{12}\Delta_1 + \lambda_{22}\Delta_2 \end{bmatrix} \qquad (19)$$

If any element in $C^{-1}\Delta_I C$ is large compared to 1, the loop transfer matrix G_pC is very different from the nominal (GC) and poor performance or even instability is expected when $\Delta_I \neq 0$. We see from (19) that controllers with large RGA-elements should always be avoided, because otherwise the closed-loop system is very sensitive to input uncertainty.

It should be added that it is the behavior of G_pC at frequencies close to the closed-loop bandwidth (where $\sigma_i(G_pC) \approx 1$) which is of primary importance for the stability of the closed-loops system. Therefore, it is particularly bad if the controller has large RGA-elements in this frequency range.

Inverse-Based Controller. To have "tight" control it is desirable to use an inverse-based controller $C(s) = c(s)G^{-1}(s)$ where $c(s)$ is a scalar. In this case $\Lambda(C) = \Lambda(G^{-1}) = \Lambda^T(G)$ and the controller will have large RGA-

elements whenever the plant has. Consequently, inverse-based controllers should always be avoided for plants with large RGA-elements. In particular, this applies to LV-control of high-purity distillation columns which always yields large RGA-elements.

Control of Plants with Large RGA-Elements. We clearly should not use an inverse-based controller for a plant with large RGA-elements. On the other hand, a diagonal controller is insensitive to uncertainty ($C^{-1}\Delta_I C = \Delta_I$), but is not able to correct for the strong directionality of the plant, which implies that performance has to be sacrificed. This is confirmed by the results presented below.

4. THE CONTROL PROBLEM

4.1 Performance and Uncertainty Specifications

The uncertainty and performance specifications are the same as those used by Skogestad and Morari (1986a).

Uncertainty. The only source of uncertainty considered is uncertainty on the manipulated inputs (L and V) with a magnitude bound

$$w_I(s) = 0.2\frac{5s+1}{0.5s+1} \tag{20}$$

The possible perturbed plants G_p are obtained by allowing any $dL = dL_c(1 \pm |w_I|)$ and $dV = dV_c(1 \pm |w_I|)$. (20) allows for an input error of up to 20% at low frequency as is used in the simulations (9). The uncertainty in (20) increases with frequency. This allows, for example, for a time delay of about 1 min in the response between the inputs, L and V, and the outputs, y_D and x_B. In practice, such delays may be caused by the flow dynamics. Therefore, although flow dynamics are not included in the models or in the simulations, they are partially accounted for in the μ-analysis and in the controller design.

Performance. We use the performance weight

$$w_p(s) = 0.5\frac{10s+1}{10s} \tag{21}$$

A particular S which exactly matches the RP-bound (15) at low frequencies and satisfies it easily at high frequencies is $S = 20s/20s+1$. This corresponds to a first-order response with closed-loop time constant 20 min.

4.2 Controllers

We will study the distillation column using the following five controllers:

1) Diagonal PI-controller.

$$C_{PI}(s) = \frac{0.01}{s}(1+75s)\begin{pmatrix} 2.4 & 0 \\ 0 & -2.4 \end{pmatrix} \tag{22}$$

The controller was tuned in order to achieve as good a performance as possible while maintaining robust stability (see Fig.3).

2) Steady-state decoupler plus two PI-controllers.

$$C_{0inv}(s) = 0.7\frac{(1+75s)}{s}G^S(0)^{-1} \tag{23}$$

This controller was tuned to achieve good nominal performance. However, the controller has large RGA-elements ($\lambda_{11}(C) = 35.1$) at all frequencies and we expect the controller to be extremely sensitive to input uncertainty.

3) Inverse-based controller based on the linear model $G_1^S(s)$ for Case 1 (Eq. 8).

$$C_{1inv}(s) = \frac{0.7}{s}G_1^S(s)^{-1} \tag{24}$$

Note that $C_{1inv}(s)$ and $G_1^S(s)^T$ have the same RGA-elements. Therefore, from Fig.2 we expect $C_{1inv}(s)$ to be sensitive to input uncertainty at low frequency, but not at high frequency.

4 and 5). μ-optimal controllers, $C_{1\mu}(s)$ and $C_{2\mu}(s)$. These controllers were obtained by minimizing $\sup_\omega \mu(N_{RP})$ for each model $G_1(s)$ and $G_2(s)$ using the input uncertainty and performance weights given above.

5. RESULTS FOR OPERATING POINT A

In this section we will study how the five controllers perform at the nominal operating point A for the two assumptions regarding condenser and reboiler holdup. The μ-plots for the 10 possible combinations are given in Fig.3. The upper solid line is $\mu(N_{RP})$ computed from (16). The

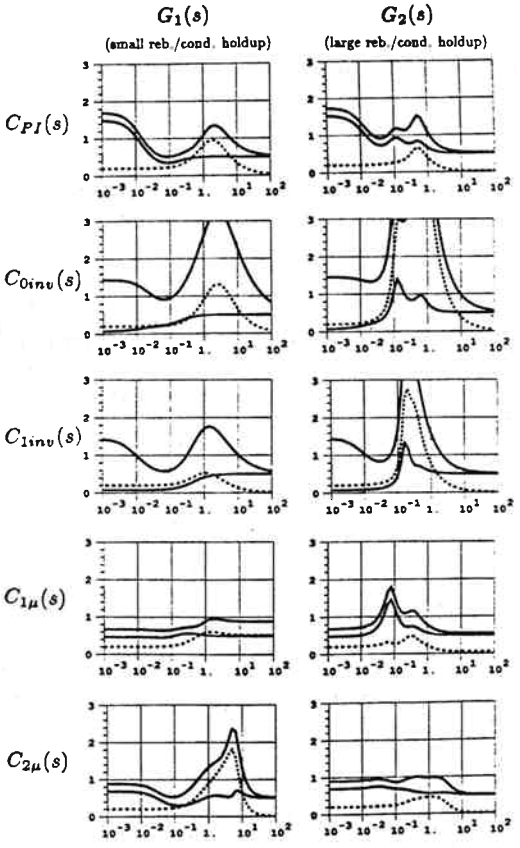

Fig. 3. μ-plots for Column A. Upper solid line: $\mu(N_{RP})$ for robust performance; Lower solid line: $\mu(N_{NP})$ for nominal performance; Dotted line: $\mu(N_{RS})$ for robust stability. The RP-, NP- or RS-requirement is satisfied if the corresponding μ-curve is less than one at all frequencies.

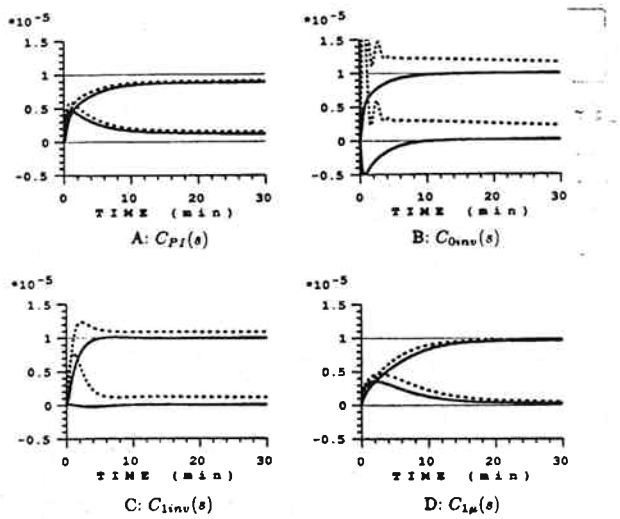

Fig. 4. Column A, Case 1. Closed-loop response to small setpoint change in y_D. Solid lines: no uncertainty; Dotted lines: 20% uncertainty on inputs L and V (Eq. 9).

lower solid line is $\mu(N_{NP}) = \bar{\sigma}((I + GC)^{-1})$. The dotted line is $\mu(N_{RS})$ (Eq. (14)). A number of interesting observations can be derived from these plots. These are presented below. In some cases the simulations in Fig.4-5 are used to support the claims.

Discussion of Controllers

$C_{PI}(s)$. The simple diagonal PI-controller performs reasonably well in all cases. μ_{NP} is higher than one at low frequency, which indicates a slow return to steady-state. This is confirmed by the simulations in Fig.5 for a feed rate disturbance; after 200 min the column has still not settled. The controller is insensitive to input uncertainty and to changes in reboiler and condenser holdup.

$C_{0inv}(s)$. This controller uses a steady-state decoupler. The nominal response is very good for Case 1 (Fig.4), but the controller is extremely sensitive to input uncertainty. In practice, this controller will yield an unstable system (Skogestad and Morari, 1986a).

$C_{1inv}(s)$. This controller gives an excellent nominal response for Case 1 (Fig.3). This is also confirmed by the simulations in Fig. 4; the response is almost perfectly decoupled with a time constant of about 1.4 min. Since the simulations are performed with the full-order model, while the controller was designed based on the simple two time-constant model, $G_1(s)$ (8), this confirms that $G_1(s)$ yields a very good approximation of the linearized plant when the reboiler and condenser holdups are small. The controller is sensitive to the input uncertainty as expected from the RGA- analysis.

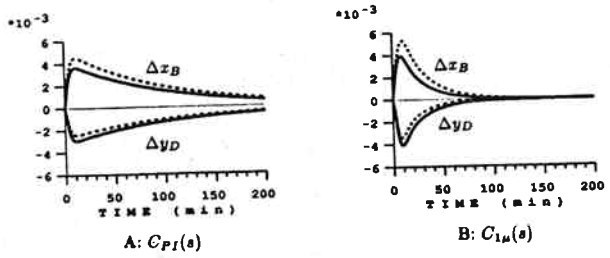

Fig. 5. Column A, Case 1. Closed-loop response to a 30% increase in feed rate. Solid lines: no uncertainty; Dotted lines: 20% uncertainty on inputs L and V (Eq. 9).

$C_{1\mu}(s)$. This is the μ-optimal controller when there is negligible holdup ($G_1(s)$), and the RP-condition is satisfied for this case since $\mu_{RP} \approx 0.95$. The nominal performance is not as good as for the inverse-based controller $C_{1inv}(s)$; we have to sacrifice nominal performance to make the system robust with respect to uncertainty. The controller shows some performance deterioration when the reboiler and condenser holdups are increased (Case 2). This is not surprising since the added holdup makes the response in y_D and x_B more sluggish.

$C_{2\mu}(s)$. This is the μ-optimal controller for the case with large reboiler and cond. holdup . $\mu_{RP} \approx 1.00$ for this case. The nominal response is good in both cases (Fig.3), but the controller is very sensitive to uncertainty when the plant is $G_1(s)$ rather than $G_2(s)$. This is clearly not desirable since changes in condenser and reboiler holdup are likely to occur during normal operation.

6. EFFECT OF NONLINEARITY (RESULTS FOR OPERATING POINT C)

6.1 Modelling

For Case 1 the following approximate model is derived when scaled compositions ($dy_D/0.1, dx_B/0.002$) are used:

$$G_{C1}^S(s) = \begin{pmatrix} \frac{16.0}{1+\tau_1 s} & \frac{16.0}{1+\tau_1 s} + \frac{0.023}{1+\tau_2 s} \\ \frac{9.3}{1+\tau_1 s} & \frac{-9.3}{1+\tau_1 s} - \frac{1.41}{1+\tau_2 s} \end{pmatrix} \quad \begin{matrix} \tau_1 = 24.5 \text{ min} \\ \tau_2 = 10 \text{ min} \end{matrix} \tag{25}$$

The steady-state gains and time constants are entirely different from those at operating point A (8). Also note that at steady state $\lambda_{11}(G(0)) = 35.1$ for Column A, but only 7.5 for Column C. However, at high-frequency the scaled plants at operating points A and C are very similar. (8) and (25) yield:

$$G_1^S(\infty) = \frac{1}{s}\begin{pmatrix} 0.45 & -0.36 \\ 0.56 & -0.65 \end{pmatrix} \quad \lambda_{11}(\infty) = 3.2 \tag{26a}$$

$$G_{C1}^S(\infty) = \frac{1}{s}\begin{pmatrix} 0.65 & -0.65 \\ 0.38 & -0.52 \end{pmatrix} \quad \lambda_{11}(\infty) = 3.7 \tag{26b}$$

Therefore, as we will show, controllers which were designed based on the model $G^S(s)$ (operating point A) do in fact perform satisfactory also when the plant is $G_C^S(s)$ rather than $G^S(s)$. The variation in gains with operating conditions is much larger if unscaled compositions are used – both at steady-state (Table 1) and at high frequencies:

$$G_1(\infty) = \frac{0.01}{s}\begin{pmatrix} 0.45 & -0.36 \\ 0.56 & -0.65 \end{pmatrix} \tag{27a}$$

$$G_{C1}(\infty) = \frac{0.01}{s}\begin{pmatrix} 6.5 & -6.5 \\ 0.08 & -0.10 \end{pmatrix} \tag{27b}$$

6.2 μ-Analysis

The μ-plots with the model $G_C^S(s)$ are shown in Fig.6. Performance is clearly worse at low frequencies at operating point C (Fig.6) than at operating point A (Fig.3). This is

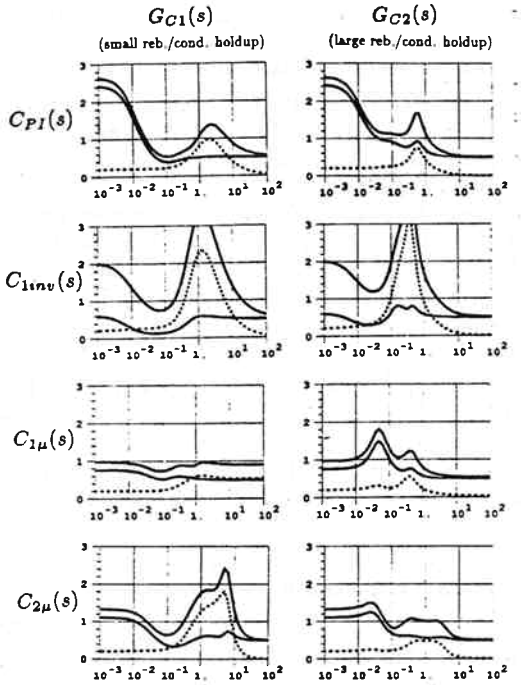

Fig. 6. μ-plots for column C. Upper solid line: $\mu(N_{RP})$; Lower solid line: $\mu(N_{NP})$; Dotted line: $\mu(N_{RS})$.

expected; the controllers were designed based on model A, and the plants are quite different at low frequencies.

The μ-optimal controller $C_{1\mu}(s)$ satisfies the robust performance requirements also at operating point C when the reboiler and condenser holdups are small. Consequently, with the use of scaled (logarithmic) compositions, a single linear controller is able to give acceptable performance at these two operating points which have quite different linear models.

6.3 Logarithmic Versus Unscaled Compositions

Fig.6 shows how controllers designed based on the scaled plant $G^S(s)$ at operating point A, perform for the scaled plant (different scaling factors!) at operating point C; this is equivalent to using logarithmic compositions (Y_D and X_B). However, we know from (27) that the plant model shows much larger changes if absolute (unscaled) compositions (y_D and x_B) are used. We therefore expect the closed-loop performance to be entirely different at operating ponts A and C when unscaled (absolute) compositions are used. This is indeed confirmed by Fig.7.

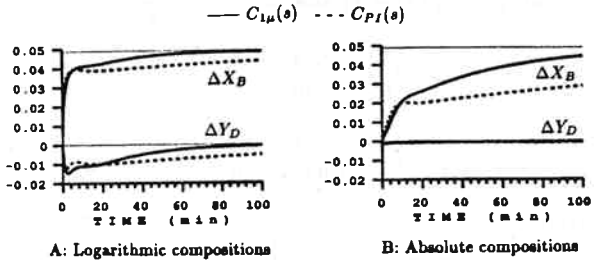

Fig. 7. Column C, Case 1. Closed-loop response to small set-point change in x_B (x_B increases from 0.002 to 0.0021)

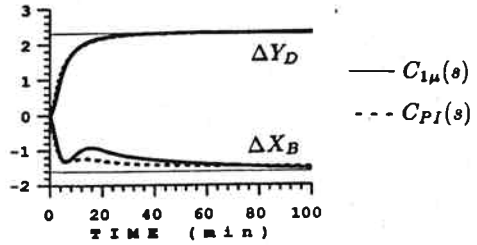

Fig. 8. Transition from operating point A to C (Case 1)

6.4 Transition from Operating Point A to C

Figure 8 shows a transition from operating point A ($Y_D = X_B = 4.605$) to operating point C ($Y_D = 2.303, X_B = 6.215$) using logarithmic compositions as controlled ouputs. The diagonal controller $C_{PI}(s)$ and the μ-optimal controller $C_{1\mu}(s)$ both yield very good responses in this particular case (However, the μ-optimal controller generally performs better at operating point C as is evident from Fig.6 and 7.).

7. CONCLUSIONS

A single linear controller is able to give satisfactory control of this high-purity column at widely different operating conditions. One reason for this is the use of logarithmic compositions which effectively counteract for the nonlinearity in the plant. However, even if a absolute compositions are used, a single linear controller performs satisfactory if the deviations from steady-state are reasonably small.

A simple diagonal controller was found to be robust with respect to model-plant mismatch, but gives a sluggish return to steady-state. This particular part of the response is improved using the μ-optimal controller. Inverse-based controllers, and in particular those based on a steady-state decoupler, are very sensitive to model-plant mismatch.

References

Bristol, E. H., "On a New Measure of Interactions for Multivariable Process Control", IEEE Trans. Automatic Control, **AC-11**, 133-134 (1966)

Doyle, J. C., "Analysis of Feedback Systems with Structured Uncertainties," IEE Proc., 129, Pt. D, **6**, 242-250 (1982).

Moczek, J. S., R. E. Otto and T. J. Williams, "Approximation Model for the Dynamic Response of Large Distillation Columns", Proc. 2nd IFAC Congress, Basel (1963).

Moore, B. C., "Principal Component Analysis in Linear System", IEEE Trans. on Automatic Control, **AC-26**, 17-32 (1981).

Skogestad, S. and M. Morari, "Control of Ill-Conditioned Plants: High- Purity Distillation", paper 74a, AIChE Annual Mtg., Miami Beach (1986a).

Skogestad, S. and M. Morari, "Implications of Large RGA-Elements on Control Performance", paper 6d, AIChE Annual Mtg., Miami Beach (1986b).

Skogestad, S. and M. Morari, "Understanding the Dynamic Behavior of Distillation Columns", submitted to Ind. & Eng. Chem. Research (1987a).

Skogestad, S. and M. Morari, "Understanding the Steady-State Behavior of Distillation Columns", in preparation (1987b).